PROCEEDINGS OF SCIENCE

The nature of the IR emission in LLAGNs at parsec scales: Does the jet dominate at low luminosities?

J. A. Fernández-Ontiveros*
Max-Planck-Institut für Radioastronomie (MPIfR), Auf dem Hügel 69, Bonn, D–53121, Germany
E-mail: jafo@mpifr.de

M. A. Prieto

Instituto de Astrofísica de Canarias (IAC), Vía Láctea s/n, La Laguna, E–38200, Spain

J. A. Acosta-Pulido

Instituto de Astrofísica de Canarias (IAC), Vía Láctea s/n, La Laguna, E–38200, Spain

S. Markoff

Astronomical Institute "Anton Pannekoek", 1098 XH Amsterdam, Netherlands

The vast majority of AGN belong to the low-luminosity class (LLAGNs) and are hard to reconcile with the unified scheme. Their low radiation efficiency and the absence of the blue bump in their spectrum, signature of the accretion disk, are usually ascribed to a radiatively inefficient accretion flow. However, these models are based on relatively poor defined SEDs, including mostly radio and X-ray but with sparse data or low-spatial resolution measurements in the IR. For a sample of 6 nearby LLAGNs, a subarcsec resolution dataset has been collected including the radio, IR, optical/UV and X-ray ranges. High-spatial resolution SEDs for this sample reveal that the mid-IR bump, indicative of the torus emission, is also missing in LLAGN. In contrast, the continuum emission is largely described by a flat/inverted radio/IR-optical spectrum with a very steep slope in the IR-to-optical ($1 < \alpha < 3$, $S_\nu \propto \nu^{-\alpha}$). This suggest that a jet component dominates the overall shape of the continuum emission for these objects.

Nuclei of Seyfert galaxies and QSOs - Central engine & conditions of star formation - seyfert2012, November 6-8, 2012
Max-Planck-Insitut für Radioastronomie (MPIfR), Bonn, Germany

*Speaker.

PoS(Seyfert 2012)028

1. Introduction

Low luminosity AGNs (LLAGNs) are the bulk of the AGN population in the near Universe, including $\sim 1/3$ of all nearby galaxies. They span a wide range in black hole (BH) mass, from Sgr A in our Galaxy ($3.3 \times 10^6\,M_\odot$, [1]) to the most massive BHs known today as M87 ($6.4 \times 10^9\,M_\odot$, [2]). For over two decades, these objects are posing a problem to the standard accretion scenario due to their low radiation efficiency and the absence, in their spectrum, of the most significant feature of the accretion disk: the blue bump [3]. Furthermore, the "torus", keystone of the Unified Model for AGNs [4] is expected to vanish at $L_{bol} \lesssim 10^{42}\,\mathrm{erg/s}$ (e.g. [5]).

The SED of LLAGNs is usually described in terms of a radiatively inefficient structure [6, 3], which explains both the low efficiency and the absence of big blue bump in these nuclei. Its main components are: *i)* an advection dominated accretion flow (ADAF), *ii)* a truncated accretion disk, and *iii)* a jet or an outflow. Overall, both ADAF- and jet-dominated models provide a good description of the continuum emission for the radio and X-ray ranges [7, 8], but cannot be probed in the IR-to-optical range using low-spatial resolution data, as the host galaxy light swamps these faint nuclei and dominates the emission. Thus, high-spatial resolution data at subarcsec scales is mandatory in order to test the nature of the emission in the IR-optical range.

2. Dataset

This work is based on a multiwavelength, high-spatial resolution dataset covering the radio, IR, optical/UV and X-ray ranges. This project is a follow-up of *The central parsecs of the nearest galaxies*[1] [9, 10], a high-spatial resolution study of the brightest and nearest Seyfert galaxies carried out at subarcsec scales with the Very Large Telescope (VLT). The objects included in the present work (Table 1) correspond to AGNs one to two order of magnitude fainter. The observations include VLT/NaCo adaptive optics imaging in the near-IR and VLT/VISIR diffraction limited imaging in the mid-IR. The dataset was completed with the highest-spatial resolution data available in the optical/UV range from the *HST* scientific archive. Nuclear fluxes were measured using aperture photometry of the unresolved component in the centre ($\lesssim 0\farcs1$), subtracting the local background around ($0\farcs2$–$0\farcs3$). In the mid-IR, *PSF* photometry was performed (see [9]). An extensive and careful search in the literature has been performed in order to complete the radio and X-ray ranges. These measurements correspond mainly to Very Large Array (VLA) and Very Long Baseline Interferometry (VLBI) in radio and *Chandra*, *XMM*-Newton and *Integral* at X-rays. Despite of their lower spatial resolution, the flux at high energies is dominated by the AGN and not by the host galaxy. A low-spatial resolution SED, based on apertures larger than few arcsec, was also compiled for comparison from NED database[2] and completed after a concise search of published measurements. The characteristics of this dataset permit us to build, for each LLAGN in the sample, a consistent SED of the same physical region, very well sampled over a wide range in wavelength.

3. The nature of the IR emission

The multiwavelength high- and low-spatial resolution SEDs allow us to: *i)* probe the genuine

[1] http://www.iac.es/project/parsec
[2] http://ned.ipac.caltech.edu/

Table 1: Galaxy sample (objects sorted by increasing distance). FWHM correspond to the size of the most compact object found in the FOV. L_{bol} is estimated from the high-spatial resolution SEDs.

Name	**D** [Mpc]	**Ref.**	**FWHM** [pc]	**1″** [pc]	**L_{bol}** [erg s^{-1}]	**Type**	**Class**
NGC 4594	9.08	[11]	3.1	44.0	1.9×10^{41}	SA(s)a	LINER 2
NGC 1097	14.2	[12]	8.9	68.8	1.9×10^{42}	SB(r′l)b	LINER 1
NGC 1386	15.3	[11]	6.7	74.2	6.6×10^{42}	SB(s)a	Sy 2
M87	16.7	[13]	9.2	81.0	1.2×10^{42}	cD	LINER 1
NGC 1052	18.0	[11]	10.5	87.3	9.3×10^{42}	E4	LINER 1.9
NGC 3169	24.7	[14]	10.9	119.7	8.1×10^{41}	SA(s)a	LINER 2

shape of the LLAGN SED; *ii)* identify the spectral ranges where the measurements might be affected by contamination from the host galaxy light; and *iii)* identify, for each object, the physical mechanisms that dominate the energy output at different wavelength ranges. Fig. 1 shows the subarcsec SEDs for the sample of LLAGNs (black dots), sorted by increasing distance. Low-spatial resolution data (grey spikes) trace the contribution of the host galaxy, which dominates the overall emission in most of the cases. For comparison, the radio-loud QSO template from [15] is also shown (orange-solid line). A self-absorbed synchrotron model (see below, [16]) has been fitted to the radio-to-UV range for each subarcsec SED (dashed line).

3.1 SEDs at parsec scales

Three main characteristics are common for all the LLAGNs in the sample (see Fig. 1): *i)* a flat radio continuum, more similar to radio-loud QSOs rather than Seyfert nuclei; *ii)* mid-IR and X-ray ranges drive the bolometric luminosity of these nuclei; and *iii)* subarcsec SEDs present a non-thermal behaviour, showing a flat/inverted radio/IR-to-optical spectrum characteristic of jet emission. We also find that the inverted IR-to-optical continuum does not follow the classical synchrotron cooling slope of about $\alpha \approx 0.7$ ($S_\nu \propto {}^{-\alpha}$) but has a much steeper spectrum, in the $1 < \alpha < 3$ range. The Sombrero galaxy (NGC 4594) shows a soft thermal bump at $\sim 1\,\mu$m.

3.2 An accretion disk/torus?

LLAGNs do not seem to fit in the standard accretion scenario, showing significantly different SEDs when compared with QSOs and Seyfert galaxies. This has been probed also for high-spatial resolution data [10, 17]. The torus, if present, is not evidenced by the continuum emission which seems to follow a non-thermal distribution. Radio-loud QSOs are more similar to LLAGNs in the radio and X-ray ranges, but the absence of a big blue bump in the latter suggest important structural differences between both classes. In contrast, recent studies based on the spectral slopes measured between optical/X-rays and mid-IR–X-rays reveal that LLAGNs present values in agreement their bright counterparts [18, 19]. These pinpoint to the presence of a classical accretion disk and a torus, respectively. In Fig. 2 we test whether this behaviour for the best sampled objects, i.e. NGC 4594, NGC 1097, M87 and NGC 1052. In blue, we show the optical/X-ray ratio found by [18] for a sample of LINERs, which have a spectral index α_{OX} between 2500 Å and 2 keV in the $0.8 < \alpha_{OX} < 1.4$ range ($S_\nu \propto \nu^{-\alpha_{OX}}$). In each case, the most favorable case within this range is plotted. In red, we show the mid-IR to X-ray correlation found by [19] for a sample of nearby

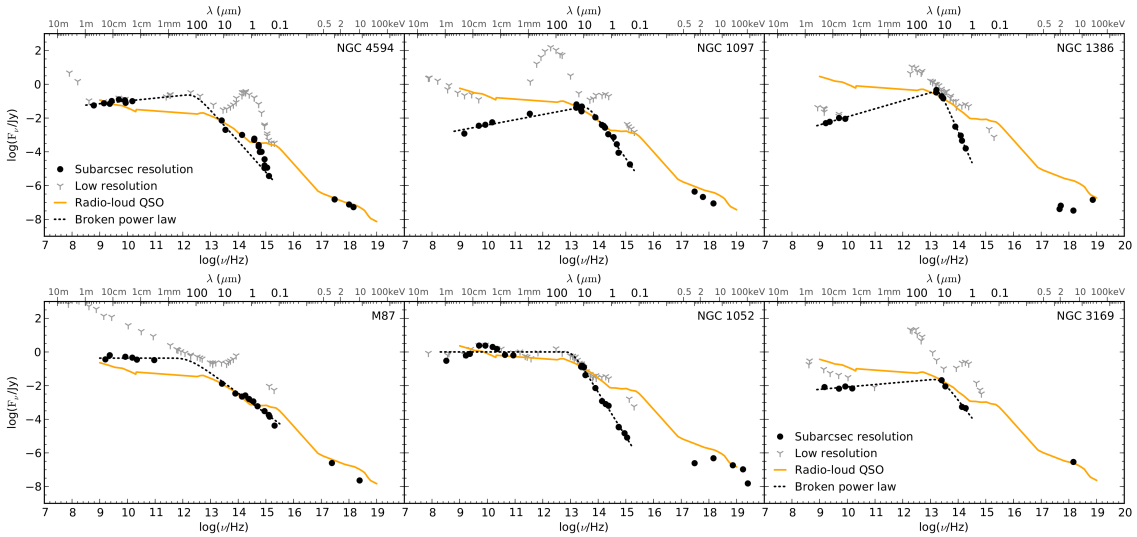

Figure 1: Subarcsec SEDs (black dots) and low-spatial resolution data (grey spikes) for the sample of LLAGNs. The orange line corresponds to the radio-loud QSO template from [15]. A self-absorbed synchrotron model, i.e. a jet, has been fitted to the radio, IR and optical/UV ranges (dashed-line).

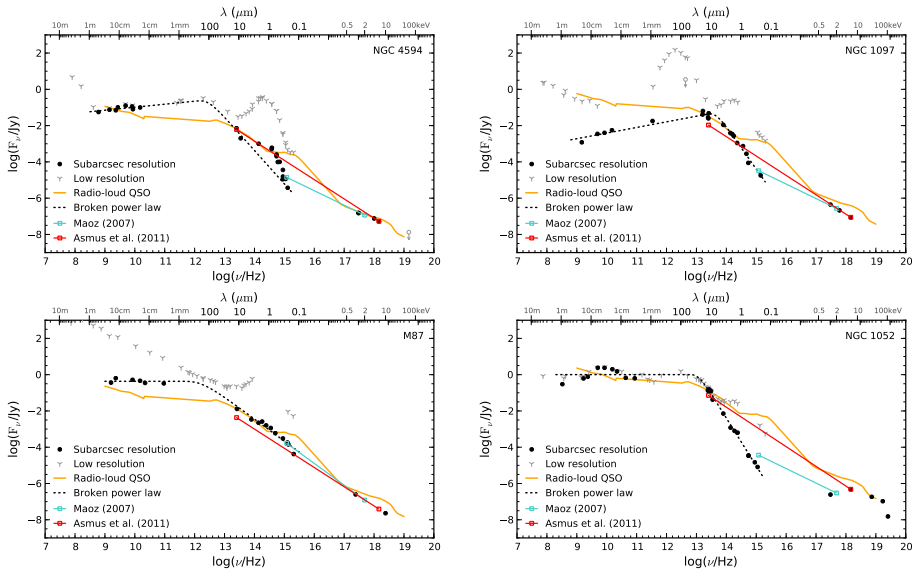

Figure 2: SEDs for the best sampled LLAGNs: NGC 4594, NGC 1097, M87 and NGC 1052 from Fig. 1. In blue, the 2500 Å/2 keV ratio from [18]. In red, the 12 μm to 2–10 keV flux correlation found by [19].

AGNs, established between the flux at 12 μm and the 2–10 keV X-ray flux. As shown by Fig. 2, the LLAGNs in our sample are in agreement with the results from [18, 19]. However, this behaviour is not produced by thermal features in the SED. In contrast, both spectral slopes are produced by a steep power-law continuum from the mid-IR to optical/UV wavelengths. The non-thermal behaviour can be well described, at first order, by a self-absorbed synchrotron model [16] (dashed line in Fig. 2), suggesting a jet as the component that drives the overall continuum emission in these objects. In Section 4 we further explore this possibility using a more detailed model of a jet.

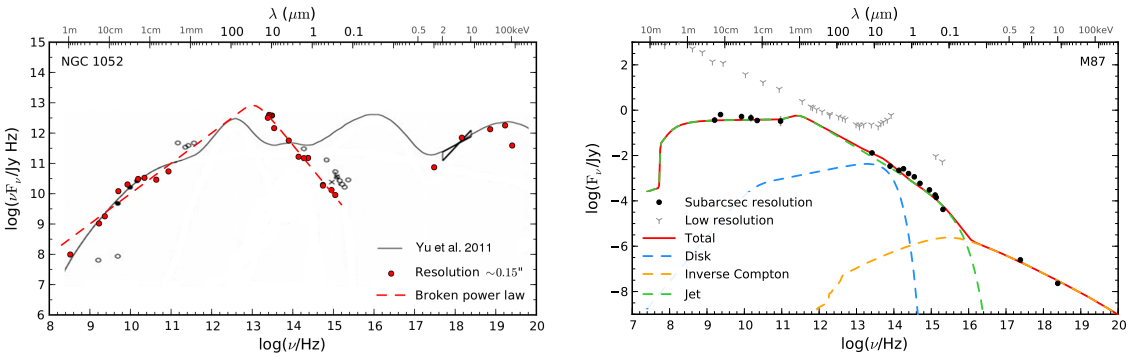

Figure 3: *Left:* ADAF model applied to NGC 1052 (in black, [7]), subarcsec SED collected in this work (red dots), and the self-absorbed synchrotron model (red-dashed line). *Right:* jet+disk dominated model from [20, 21], applied to the subarcsec SED of M87. Individual components of the model are also plotted.

Nonetheless, one should keep in mind that these spectral ratios are not able to discriminate bright AGNs with strong thermal contributions in the mid-IR (torus) and the optical/UV (accretion disk) from LLAGNs dominated by a steep non-thermal continuum as those included in our work.

4. Inflow and Outflow

ADAF and jet models in the literature are usually based on relatively poorly defined SEDs with insufficient spatial resolution and/or wavelength coverage. In particular, low-resolution data in the IR and, thus, upper limits in this range, are common reference. Our subarcsec SEDs allow us to probe the models in this range. Left panel in Fig. 3 shows an ADAF fit for the case of NGC 1052 (in black, [7]). The spectral features predicted by ADAF models, i.e. bumps in the millimetric to X-ray range, are not detected in any of the LLAGNs of the sample. The mid-IR to optical/UV continuum in NGC 1052 largely departs from the ADAF prediction, following a very steep power law distribution ($\alpha = 2.7$). The right panel in Fig. 3 shows a fit of the jet+disk dominated model developed by [20, 21] to the SED of M87. Data for M87 are not simultaneous but are carefully selected from quiescent periods in which the core was in a low state of activity. The jet emission can explain the overall shape of the continuum emission for this LLAGN. Still, there are gaps in the SED that should be sampled (e.g. the submillimetric range with ALMA) in order to test the validity of these models and constrain the large number of parameters involved in the fit.

5. Summary

The importance of LLAGNs lies in the fact that they permit to explore the limits of the classical picture for active nuclei. At very low luminosities the torus is expected to vanish and the classical accretion scenario changes, giving way to a radiatively inefficient structure. As a consequence of the changes in the inner structure, the SEDs of LLAGNs present important differences with regard to the bright class. Subarcsec SEDs collected for a sample of 6 nearby LLAGNs permit us to avoid the contamination from the host galaxy light and directly test the processes that dominate the emission for these objects. The torus and the accretion disk, if present, are not detected in the

subarcsec SEDs. Most of the nuclei in the sample are well described by a flat/inverted radio/IR-to-optical continuum, suggesting that a jet is driving the energy output. However, the inverted IR-to-optical continuum does not follow the classical synchrotron cooling slope and show a much steeper spectrum ($1 < \alpha < 3$).

References

[1] Schödel R, Ott T, Genzel R, Eckart A, Mouawad N and Alexander T 2003 ApJ **596** 1015–1034 (*Preprint* arXiv:astro-ph/0306214)

[2] Gebhardt K and Thomas J 2009 ApJ **700** 1690–1701 (*Preprint* 0906.1492)

[3] Ho L C 2008 ARA&A **46** 475–539 (*Preprint* 0803.2268)

[4] Antonucci R 1993 ARA&A **31** 473–521

[5] Hönig S F and Beckert T 2007 MNRAS **380** 1172–1176

[6] Narayan R 2005 Ap&SS **300** 177–188 (*Preprint* arXiv:astro-ph/0411385)

[7] Yu Z, Yuan F and Ho L C 2011 ApJ **726** 87 (*Preprint* 1011.1962)

[8] Falcke H, Körding E and Markoff S 2004 A&A **414** 895–903 (*Preprint* arXiv:astro-ph/0305335)

[9] Reunanen J, Prieto M A and Siebenmorgen R 2010 MNRAS **402** 879–894 (*Preprint* 0911.2112)

[10] Prieto M A, Reunanen J, Tristram K R W, Neumayer N, Fernandez-Ontiveros J A, Orienti M and Meisenheimer K 2010 MNRAS **402** 724–744 (*Preprint* 0910.3771)

[11] Jensen J B, Tonry J L, Barris B J, Thompson R I, Liu M C, Rieke M J, Ajhar E A and Blakeslee J P 2003 ApJ **583** 712–726 (*Preprint* arXiv:astro-ph/0210129)

[12] Tully R B, Rizzi L, Shaya E J, Courtois H M, Makarov D I and Jacobs B A 2009 AJ **138** 323–331

[13] Blakeslee J P, Jordán A, Mei S, Côté P, Ferrarese L, Infante L, Peng E W, Tonry J L and West M J 2009 ApJ **694** 556–572 (*Preprint* 0901.1138)

[14] Mandel K S, Wood-Vasey W M, Friedman A S and Kirshner R P 2009 ApJ **704** 629–651 (*Preprint* 0908.0536)

[15] Elvis M, Wilkes B J, McDowell J C, Green R F, Bechtold J, Willner S P, Oey M S, Polomski E and Cutri R 1994 ApJS **95** 1–68

[16] Marscher A P and Gear W K 1985 ApJ **298** 114–127

[17] Mason R E, Lopez-Rodriguez E, Packham C, Alonso-Herrero A, Levenson N A, Radomski J, Ramos Almeida C, Colina L, Elitzur M, Aretxaga I, Roche P F and Oi N 2012 AJ **144** 11 (*Preprint* 1205.0029)

[18] Maoz D 2007 MNRAS **377** 1696–1710 (*Preprint* arXiv:astro-ph/0702292)

[19] Asmus D, Gandhi P, Smette A, Hönig S F and Duschl W J 2011 A&A **536** A36 (*Preprint* 1109.4873)

[20] Markoff S, Nowak M A and Wilms J 2005 ApJ **635** 1203–1216 (*Preprint* arXiv:astro-ph/0509028)

[21] Markoff S, Nowak M, Young A, Marshall H L, Canizares C R, Peck A, Krips M, Petitpas G, Schödel R, Bower G C, Chandra P, Ray A, Muno M, Gallagher S, Hornstein S and Cheung C C 2008 ApJ **681** 905–924 (*Preprint* 0804.0344)